

## Dynamic array of dark optical traps

Vincent Ricardo Daria, Peter John Rodrigo, and Jesper Glückstad<sup>a)</sup>

*Optics and Fluid Dynamics Department, Risø National Laboratory, P.O. Box 49, DK-4000 Roskilde, Denmark*

(Received 28 July 2003; accepted 17 November 2003)

A dynamic array of dark optical traps is generated for simultaneous trapping and arbitrary manipulation of multiple low-index microstructures. The dynamic intensity patterns forming the dark optical trap arrays are generated using a nearly loss-less phase-to-intensity conversion of a phase-encoded coherent light source. Two-dimensional input phase distributions corresponding to the trapping patterns are encoded using a computer-programmable spatial light modulator, enabling each trap to be shaped and moved arbitrarily within the plane of observation. We demonstrate the generation of multiple dark optical traps for simultaneous manipulation of hollow “air-filled” glass microspheres suspended in an aqueous medium. © 2004 American Institute of Physics.

[DOI: 10.1063/1.1642752]

Optical trapping is a well-documented method for non-invasive manipulation of micro- and nanoscale particles.<sup>1,2</sup> Conventional optical trapping techniques that make use of a focused Gaussian beam ( $TEM_{00}$ ) can be used to trap transparent particles with a higher refractive index than the surrounding medium. The balance of the counteracting forces induced by a focused  $TEM_{00}$  beam on a high index particle, i.e., the gradient force and the scattering force, results in a confinement of the object within the focal region.<sup>3</sup>

Micron-sized low-index particles, metal fragments, or strongly absorbing particles, however, are difficult to handle using conventional optical trapping techniques because the balance of the light induced forces is not achieved. The predominance of either the scattering/absorption force or the net effect of the gradient force repels these types of particles out of the region of stronger light intensity. In order to confine and manipulate such micron-sized particles, dark optical traps have to be applied. Several techniques to produce dark optical traps have been realized by high-speed deflectable mirrors that scan a beam in a circular locus,<sup>4</sup> Laguerre–Gaussian beams from computer-generated holograms,<sup>5–7</sup> and line patterns from interfering plane waves.<sup>8</sup> These techniques work well for generating a single dark optical trap. While it is theoretically possible to increase the number of traps for some of these techniques, their implementations would require sophisticated optical components and intricate setups that still do not guarantee efficient multiple trapping in combination with a fully dynamic and independent manipulation functionality.

This work demonstrates the use of a dynamic array of dark optical traps for simultaneous trapping and arbitrary manipulation of multiple “air-filled” hollow glass microspheres suspended in an aqueous medium. The hollow microspheres have an effective refractive index lower than that of the surrounding medium (e.g., water) and as a consequence they are readily repelled by a focused  $TEM_{00}$  beam.<sup>9</sup> The experiments described here substantiate the flexibility and unique functionalities of a previously reported

technique<sup>10,11</sup> to achieve complex beam shaping functionalities suitable for trapping a variety of microstructures. Optical manipulation of a wide range of microstructures is a promising tool for controlling microfluidic components as well as alignment of components in micro-optomechanical systems.<sup>12,13</sup> In some cases, the scattering and absorption properties as well as the effective refractive indices of specially fabricated microstructures<sup>14,15</sup> are not known or vary differently for a mixture of particles. Thus, the applicability of multiple-beam optical manipulator depends on having advanced beam-shaping functionalities that can flexibly and rapidly adapt to specific particle characteristics.

The dynamic multiple dark optical traps are generated by a phase-encoded incident light source that undergoes a spatial phase filtering at the Fourier plane of a 4- $f$  lens imaging system as shown in Fig. 1. The intensity,  $I(x',y')$ , in relation to the input phase pattern,  $\phi(x,y)$ , can be expressed as<sup>16</sup>

$$I(x',y') = |\exp(i\tilde{\phi}(x',y'))\text{circ}(r'/\Delta r) + g(r')|\bar{\alpha}|(\exp(i\theta) - 1)|^2 \quad (1)$$

with

$$\begin{aligned} \bar{\alpha} &= A^{-1} \iint_A \exp(i\phi(x,y)) dx dy = |\bar{\alpha}| \exp(i\phi_{\bar{\alpha}}), \\ \tilde{\phi}(x,y) &= \phi(x,y) - \phi_{\bar{\alpha}}, \\ r' &= \sqrt{x'^2 + y'^2}. \end{aligned} \quad (2)$$

The complex valued and object dependent term,  $\bar{\alpha}$ , is the spatial average of the input wave front with absolute value  $|\bar{\alpha}|$  and phase  $\phi_{\bar{\alpha}}$ . The phase pattern,  $\phi(x,y)$ , is addressed on a phase-only spatial light modulator (SLM) truncated with a circular aperture with area  $A = \pi(\Delta r)^2$ . A spatial phase-only filter placed at the Fourier plane of the 4- $f$  lens sets the phase shift,  $\theta$ , of the on-axis component of the phase-encoded light. The interference between the phase-shifted on-axis term and the unfiltered phase information shapes the output intensity distribution,  $I(x',y')$ , matching the requirements for the creation of dark optical traps. The

<sup>a)</sup>Electronic mail: jesper.gluckstad@risoe.dk

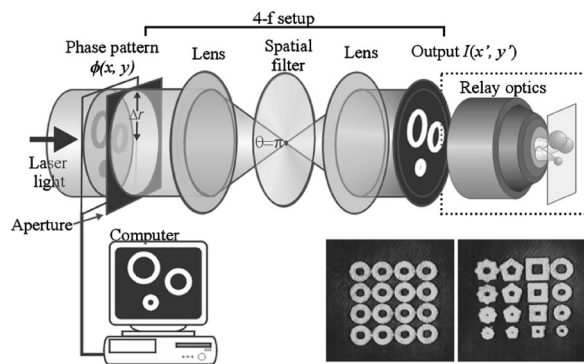


FIG. 1. The setup for generating dynamic multiple dark optical traps. The insets show various dark optical trap configurations in an array of  $4 \times 4$  and with arbitrary geometries.

output intensity distribution is also dependent on the term,  $g(r')$ , which describes the spatial profile of the synthetic reference wave,<sup>16</sup> diffracted from the phase-step formed by the on-axis filtering region. In order to obtain an optimized phase-to-intensity conversion, the generalized phase contrast (GPC)<sup>17</sup> method prescribes a unique relationship between the term,  $g(r'=0) = K$ , and  $\bar{\alpha}$  such that it satisfies the following condition for optimal visibility and light efficiency:

$$K|\bar{\alpha}| = |2 \sin(\theta/2)|^{-1}. \quad (3)$$

In the current experimental setup, a 200 mW diode laser operating at a wavelength  $\lambda = 830$  nm is expanded, collimated, and directed onto the surface of a reflection-type phase-only SLM. The SLM is a parallel-aligned nematic liquid crystal type (Hamamatsu Photonics), which can modulate phase in the range  $[0:2\pi]$  at 830 nm wavelength. The input phase pattern  $\phi(x, y)$  is optically encoded at the SLM by a  $480 \times 480$  pixel resolution liquid crystal projector controlled by the video output of a computer. At the Fourier plane of the 4- $f$  lens, a 30- $\mu\text{m}$ -diam spatial phase-only filter introduces a  $\theta = \pi$  phase shift to the on-axis focused light. This filter is fabricated by depositing a  $\lambda/2$  thick photoresist protrusion on a glass optical flat. For a fixed prefabricated filter, the condition for optimum phase-to-intensity conversion identified by Eq. (3) is achieved by adjusting the radius,  $\Delta r$ , of the circular aperture after the SLM. Hence, such a condition prescribed by the GPC method can be understood as the relationship of the on-axis spatial filtering region with the spatial frequency distribution describing the focused light spot.

With the condition for optimum phase-to-intensity conversion satisfied,  $I(x', y')$  is generated at the output plane after the 4- $f$  lens. The insets in Fig. 1 show various dark optical traps in an array of  $4 \times 4$  and arbitrary geometries measured at the output plane of the 4- $f$  lens. Relay optics and other conditioning components are used to scale  $I(x', y')$  for trapping of microstructures. The relay optics, composed of a lens and a microscope objective lens (numerical aperture = 1.4 oil immersion; also used to project images of the trapped particles to a charge-coupled device camera), sets the demagnification of four pixels ( $\sim 40 \mu\text{m}/\text{pixel}$ ) to a spot size of  $\sim 1 \mu\text{m}$  in the trapping plane. The estimated efficiency of the system of only 35% can be attributed mainly to losses encountered by the use of inappropriate antireflection coat-

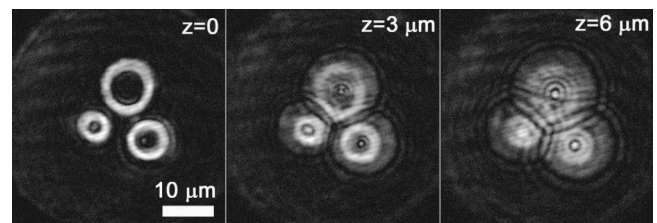


FIG. 2. Measured intensity distribution of three dark optical traps having different diameters. Images were taken at (a) the focal plane and (b) and (c) at out-of-focus planes. Each particle is effectively trapped within the dark space region of the corresponding trap.

ings for the objective lens at the current operating wavelength. Further details of the experimental setup have been discussed in a previous work.<sup>10</sup>

Figure 2 shows the intensity distribution corresponding to the dark optical traps at: (a) the focal plane and (b) and (c) the out-of-focus planes. These images were obtained by positioning a mirror at three different axial positions  $z = 0, 3$ , and  $6 \mu\text{m}$ , from the focal plane of the objective lens. To demonstrate the flexibility of the system, dark optical traps of different sizes were created. As the mirror is displaced from the focal plane of the objective lens, the intensity pattern changes with an emerging bright spot at the center of each dark trap. This suggests a strong intensity gradient slightly off the focal plane and along the optical axis, thus realizing dark optical traps within a three-dimensional region.

It is important to note that a dark optical trap or an optical vortex produced by a computer-generated hologram produces a cone of dark region surrounded by the bright portion of the focused light. Implementing an optical vortex for trapping low-index particles therefore relies on the precise balance of the scattering and gradient forces with the particle trapped slightly off the focal plane.<sup>5</sup> Hence, the trapping position along the optical axis, where the particle encounters a considerable gradient force to counteract the forward scattering force of light, strongly depends on the size of the trapped particle. This limitation is not a point of concern in our implementation since the particles are trapped in the dark space around the three-dimensional focal region. Hence, the trapped particles can be observed directly and with no out-of-focus blurring by the same objective lens used for projecting the trapping beams.

Trapping and dynamic manipulation of multiple particles having lower refractive indices are demonstrated using hollow glass microspheres (Polysciences Inc.) suspended in water contained in a 30- $\mu\text{m}$ -thick sample cell. An ample amount of surfactant was added to the diluted microsphere solution to prevent the glass spheres from sticking to the glass boundaries of the sample cell. The diameters of the spheres vary from 2 to 20  $\mu\text{m}$  and the thickness of the glass shells is approximately 1  $\mu\text{m}$ . Hence, the average index of refraction for smaller particles ( $< 8 \mu\text{m}$ ) approaches that of the glass shells. For this reason, trapping and manipulation of low-index particles is only demonstrated for particles with diameters within the size range 10–12  $\mu\text{m}$ , since the average index of refraction remains substantially lower than that of the surrounding medium. To position the particles into their corresponding dark optical traps, the particles are first

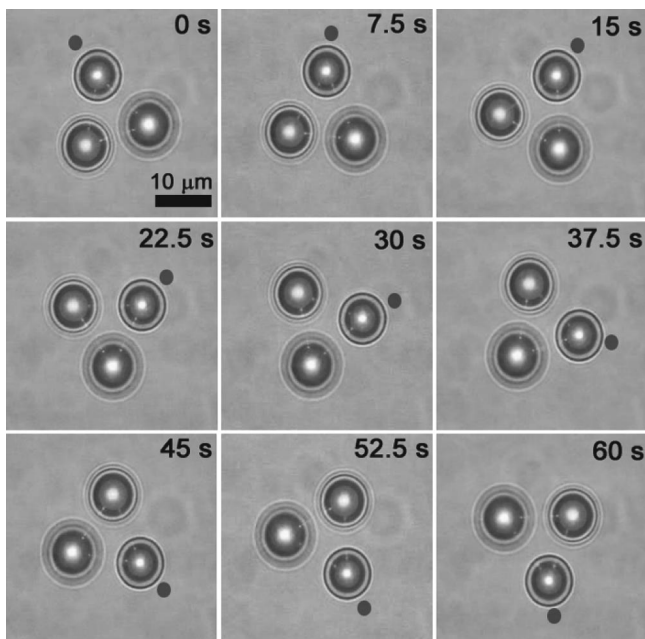


FIG. 3. Image sequence showing simultaneous trapping and dynamic manipulation of three hollow glass microspheres rotating in a clockwise direction. The spheres have different sizes with diameters in the range 10–12  $\mu\text{m}$ . Particle movement is visualized with a black spot that translates more than half a revolution in 60 s. See EPAPS Ref. 18.

brought into the viewing region. The ability to dynamically encode phase patterns at the SLM allows each dark trap to be independently switched on and off until the traps coincide with the position of the particles. Once all the traps have been filled with particles, the sample stage is moved to isolate the trapped particles from the freely moving particles.

Figure 3 shows an image sequence demonstrating simultaneous trapping of three hollow spheres rotating in a clockwise direction. The laser diode operating at 830 nm wavelength provides a single-mode Gaussian beam profile with a maximum power of 200 mW. Operating the laser within a reasonable power level and considering the significant 65% wavelength-related losses of the system, the operational power at the trapping plane is estimated to be only 30 mW. This power is distributed among the traps in proportion to the area that each trap illuminates. The system can, however, be straightforwardly upgraded to trap a larger number of low-index particles and to move them at greater speed by using proper antireflection coatings for the optics or by simply increasing the available input power provided that it does not go beyond the tolerance limits of the SLM ( $\sim 3$  W for most SLMs). With the current input laser power, the particles are manipulated with an average speed of  $0.5 \mu\text{m s}^{-1}$ . In Fig. 3, one particle is tracked with a black spot to visualize the movement of more than half a revolution in 60 s. It is important to note that the maximum intensity at the trapping

plane is maintained even for a dynamically changing trapping configuration as long as the fractional area of the dark and bright regions is kept within a certain ratio.<sup>16</sup> As such, increasing the lateral size of a trap directly relates to an increase in overall optical power for that trap.

We have demonstrated the use of a dynamic array of dark optical traps for parallel trapping and manipulation of low-index microstructures. This experiment confirms the unique functionalities of an optical trapping approach based on a light efficient phase-to-intensity conversion technique. Using a computer-programmable SLM to encode phase patterns corresponding to the trapping configuration enables each trap to have a user-defined profile and arbitrary spatial position at the plane of observation. Thus, our method offers an advanced user-interactive optical trapping functionality and high adaptability to specific properties of a mixture of microstructures. These functionalities are particularly essential when strongly absorptive particles and biological specimens are subjected to optical trapping. In addition, the spatial profile of the dark optical traps can be reconfigured to mimic the contours of the microstructures under direct observation and thereby strongly minimize the optical damage due to absorptive heating.

This work has been funded as part of an award from the Danish Technical Scientific Research Council. The authors acknowledge the assistance of T. Hara and Y. Kobayashi of Hamamatsu Photonics for the operation of the SLM.

<sup>1</sup>A. Ashkin, *Phys. Rev. Lett.* **24**, 156 (1970).

<sup>2</sup>A. Ashkin, J. M. Dziedzic, J. E. Bjorkholm, and S. Chu, *Opt. Lett.* **11**, 288 (1986).

<sup>3</sup>A. Ashkin and J. M. Dziedzic, *Appl. Phys. Lett.* **24**, 586 (1974).

<sup>4</sup>K. Sasaki, M. Koshioka, H. Misawa, N. Kitamura, and H. Masuhara, *Appl. Phys. Lett.* **60**, 807 (1992).

<sup>5</sup>H. He, N. R. Heckenberg, and H. Rubinsztein-Dunlop, *J. Mod. Opt.* **42**, 217 (1995).

<sup>6</sup>K. T. Gahagan and G. A. Swartzlander, *Opt. Lett.* **21**, 827 (1996).

<sup>7</sup>D. Ganic, X. Gan, M. Gu, M. Hain, S. Somalingam, S. Stankovic, and T. Tschudi, *Opt. Lett.* **27**, 1351 (2002).

<sup>8</sup>M. P. MacDonald, L. Paterson, W. Sibbett, K. Dholakia, and P. E. Bryant, *Opt. Lett.* **26**, 863 (2001).

<sup>9</sup>K. T. Gahagan and G. A. Swartzlander, *J. Opt. Soc. Am. B* **15**, 524 (1998).

<sup>10</sup>R. L. Eriksen, V. R. Daria, and J. Glückstad, *Opt. Express* **10**, 597 (2002).

<sup>11</sup>P. J. Rodrigo, R. L. Eriksen, V. R. Daria, and J. Glückstad, *Opt. Express* **10**, 1550 (2002).

<sup>12</sup>A. Terray, J. Oakley, and D. W. M. Marr, *Science* **296**, 1841 (2002).

<sup>13</sup>E. Higurashi, R. Sawada, and T. Ito, *Appl. Phys. Lett.* **73**, 3034 (1998).

<sup>14</sup>S. Kawata, H. B. Sun, T. Tanaka, and K. Takada, *Nature (London)* **412**, 697 (2001).

<sup>15</sup>S. Maruo, O. Nakamura, and S. Kawata, *Opt. Lett.* **22**, 132 (1997).

<sup>16</sup>J. Glückstad and P. C. Mogensen, *Appl. Opt.* **40**, 268 (2001).

<sup>17</sup>J. Glückstad, U.S. Patent No. 6,011,874 (January 2000).

<sup>18</sup>See EPAPS Document No. E-APPLAB-84-048403 for supplemental movie sequence. A direct link to this document may be found in the online article's HTML reference section. The document may also be reached via the EPAPS homepage (<http://www.aip.org/pubservs/epaps.html>) or from <ftp.aip.org> in the directory /epaps/. See the EPAPS homepage for more information.